

MAVIPER: Learning Decision Tree Policies for Interpretable Multi-Agent Reinforcement Learning

Stephanie Milani^{*1}, Zhicheng Zhang^{*2}, Nicholay Topin¹, Zheyuan Ryan Shi¹,
Charles Kamhoua³, Evangelos E. Papalexakis⁴, and Fei Fang¹

¹ Carnegie Mellon University smilani@andrew.cmu.edu

² Shanghai Jiao Tong University

³ Army Research Lab

⁴ University of California, Riverside

Abstract. Many recent breakthroughs in multi-agent reinforcement learning (MARL) require the use of deep neural networks, which are challenging for human experts to interpret and understand. On the other hand, existing work on interpretable RL has shown promise in extracting more interpretable decision tree-based policies, but only in the single-agent setting. To fill this gap, we propose the first set of algorithms that extract interpretable decision-tree policies from neural networks trained with MARL. The first algorithm, IVIPER, extends VIPER, a recent method for single-agent interpretable RL, to the multi-agent setting. We demonstrate that IVIPER can learn high-quality decision-tree policies for each agent. To better capture coordination between agents, we propose a novel centralized decision-tree training algorithm, MAVIPER. MAVIPER jointly grows the trees of each agent by predicting the behavior of the other agents using their anticipated trees, and uses resampling to focus on states that are critical for its interactions with other agents. We show that both algorithms generally outperform the baselines and that MAVIPER-trained agents achieve better-coordinated performance than IVIPER-trained agents on three different multi-agent particle-world environments.

Keywords: interpretability · explainability · multi-agent reinforcement learning

1 Introduction

Multi-agent reinforcement learning (MARL) is a promising technique for solving challenging problems, such as air traffic control [5], train scheduling [24], cyber defense [20], and autonomous driving [4]. In many of these scenarios, we want to train a *team* of cooperating agents. Other settings, like cyber defense, involve an adversary or set of adversaries with goals that may be at odds with the team of

* Equal contribution

defenders. To obtain high-performing agents, most of the recent breakthroughs in MARL rely on neural networks (NNs) [9,32], which have thousands to millions of parameters and are challenging for a person to interpret and verify. Real-world risks necessitate learning *interpretable* policies that people can inspect and verify before deployment, while still performing well at the specified task and being robust to a variety of attackers (if applicable).

Decision trees [31] (DTs) are generally considered to be an *intrinsically* interpretable model family [25]: sufficiently small trees can be contemplated by a person at once (*simulatability*), have subparts that can be intuitively explained (*decomposability*), and are verifiable (*algorithmic transparency*) [17]. In the RL setting, DT-like models have been successfully used to represent transition models [37], reward functions [7], value functions [30,40], and policies [22]. Although learning DT policies for interpretability has been investigated in the single-agent RL setting [22,29,34], it has not been explored in the multi-agent setting.

To address this gap, we propose two algorithms, IVIPER and MAVIPER, which combine ideas from model compression and imitation learning to learn DT policies in the multi-agent setting. Both algorithms extend VIPER [2], which extracts DT policies for single-agent RL. IVIPER and MAVIPER work with most existing NN-based MARL algorithms: the policies generated by these algorithms serve as “expert policies” and guide the training of a set of DT policies.

The main contributions of this work are as follows. First, we introduce the IVIPER algorithm as a novel extension of the single-agent VIPER algorithm to multi-agent settings. IVIPER learns DT policies that achieve high individual performance in the multi-agent setting. Second, to better capture coordination between agents, we propose a novel centralized decision-tree training algorithm, MAVIPER. MAVIPER jointly grows the trees of each agent by predicting the behavior of the other agents in the environment using their anticipated trees. To train each agent’s policy, MAVIPER uses resampling to find states that are considered critical for its interactions with other agents. We show that MAVIPER-trained agents achieve better coordinated performance than IVIPER-trained agents on three different multi-agent particle-world environments.

2 Background and Preliminaries

We focus on the problem of learning interpretable DT policies in the multi-agent setting. We first describe the formalism of our multi-agent setting. We then discuss DT policies and review the single-agent version of VIPER.

2.1 Markov Games and MARL Algorithms

In MARL, agents act in an environment defined by a Markov game [18,35]. A Markov game for N agents consists of a set of states \mathcal{S} describing all possible configurations for all agents, the initial state distribution $\rho : \mathcal{S} \rightarrow [0, 1]$, and the set of actions $\mathcal{A}_1, \dots, \mathcal{A}_N$ and observations $\mathcal{O}_1, \dots, \mathcal{O}_N$ for each agent $i \in [N]$. The goal of each agent is to maximize its own total expected return $R_i =$

$\sum_{t=0}^{\infty} \gamma^t r_i^t$, where γ is the discount factor that weights the relative importance of future rewards. To accomplish this goal, each agent selects actions using a policy $\pi_{\theta_i} : \mathcal{O}_i \rightarrow \mathcal{A}_i$. After the agents simultaneously execute their actions \vec{a} in the environment, the environment produces the next state according to the state transition function $P : \mathcal{S} \times \mathcal{A}_1 \times \dots \times \mathcal{A}_N \rightarrow \mathcal{S}$. Each agent i receives reward according to a reward function $r_i : \mathcal{S} \times \mathcal{A}_i \rightarrow \mathbb{R}$ and a private observation correlated with the state $o_i : \mathcal{S} \rightarrow \mathcal{O}_i$. Each observation o_i consists of a vector of *features*, which are explanatory variables that describe o_i .

Given a policy profile $\pi = (\pi_1, \dots, \pi_N)$, agent i 's value function is defined as: $V_i^\pi(s) = r_i + \gamma \sum_{s' \in \mathcal{S}} P(s, \pi_1(o_1), \dots, \pi_N(o_N), s') V_i^\pi(s')$ and state-action value function is: $Q_i^\pi(s, a_1, \dots, a_N) = r_i + \gamma \sum_{s' \in \mathcal{S}} P(s, a_1, \dots, a_N, s') V_i^\pi(s')$. We refer to a policy profile excluding agent i as π_{-i} .

Recent MARL algorithms fall into two categories: value-based [32,36,38] and actor-critic [10,15,19,45]. Value-based methods often approximate Q -functions for individual agents in the form of $Q_i^\pi(o_i, a_i)$ and derive the policies π_i by taking actions with the maximum Q -values. In contrast, actor-critic methods often follow the centralized training and decentralized execution (CTDE) paradigm [27]. These techniques train agents in a centralized manner, enabling them to leverage information beyond their private observation during training. However, agents must behave in a decentralized manner during execution. Each agent i uses a centralized critic network Q_i^π , which takes as input some state information x (including the observations of all agents) and the actions of all agents a_1, \dots, a_N . This assumption addresses the stationarity issue in MARL training: without access to the actions of other agents, the environment appears non-stationary from the perspective of any one agent. Each agent i also has a policy network π_i that takes as input its observation o_i .

2.2 Decision Tree Policies

DTs are tree-like models that recursively partition the input space along a specific feature using a cutoff value. These models produce axis-parallel partitions. Internal nodes are the intermediate partitions, and leaf nodes are the final partitions. When used to represent policies, the internal nodes represent the features and values of the input state that the agent uses to choose its action, and the leaf nodes correspond to chosen actions given some input state.

2.3 VIPER

VIPER [2] extracts DT policies for a finite-horizon Markov decision process given an *expert* policy trained using any single-agent RL algorithm. It combines ideas from model compression [6,12] and imitation learning [1] — specifically, a variation of the DAGGER algorithm [33]. It uses a high-performing deep NN that approximates the state-action value function to guide the training of a DT policy.

VIPER trains a DT policy $\hat{\pi}^m$ in each iteration m ; the final output is the best policy among all iterations. More concretely, in iteration m , it samples

Algorithm 1 IVIPER in Multi-Agent Setting

Input: (X, A, P, R) , π^* , $Q^{\pi^*} = (Q_1^{\pi^*}, \dots, Q_N^{\pi^*})$, K, M **Output:** $\hat{\pi}_1, \dots, \hat{\pi}_N$

- 1: **for** $i=1$ to N **do**
 - 2: Initialize dataset $\mathcal{D}_i \leftarrow \emptyset$ and policy $\hat{\pi}_i^0 \leftarrow \pi_i^*$
 - 3: **for** $m = 1$ to M **do**
 - 4: Sample K trajectories: $\mathcal{D}_i^m \leftarrow \{(x, \pi_1^*(o_1), \dots, \pi_N^*(o_N)) \sim d^{\hat{\pi}_i^{m-1}, \pi_i^*}\}$
 - 5: Aggregate dataset $\mathcal{D}_i \leftarrow \mathcal{D}_i \cup \mathcal{D}_i^m$
 - 6: Resample dataset according to loss:
 $\mathcal{D}'_i \leftarrow \{(x, \vec{a}) \sim p((x, \vec{a})) \propto \tilde{l}_i(x) \mathbb{1}[(x, \vec{a}) \in \mathcal{D}_i]\}$
 - 7: Train decision tree $\hat{\pi}_i^m \leftarrow \text{TrainDecisionTree}(\mathcal{D}'_i)$
 - 8: Get best policy $\hat{\pi}_i \leftarrow \text{BestPolicy}(\hat{\pi}_i^1, \dots, \hat{\pi}_i^M, \pi_i^*)$
 - 9: **return** Best policies for each agent $\hat{\pi} = (\hat{\pi}_1, \dots, \hat{\pi}_N)$
-

K trajectories $\{(s, \hat{\pi}^{m-1}(s)) \sim d^{\hat{\pi}^{m-1}}\}$ following the DT policy trained at the previous iteration. Then, it uses the expert policy π^* to suggest actions for each visited state, leading to the dataset $D^m = \{(s, \pi^*(s)) \sim d^{\hat{\pi}^{m-1}}\}$ (Line 4, Alg. 3). VIPER adds these relabeled experiences to a dataset \mathcal{D} consisting of experiences from previous iterations. Let V^{π^*} and Q^{π^*} be the state value function and state-action value function given the expert policy π^* . VIPER resamples points $(s, a) \in \mathcal{D}$ according to weights:

$$\tilde{l}(s) = V^{\pi^*}(s) - \min_{a \in A} Q^{\pi^*}(s, a). \quad (1)$$

See Algorithm 3 in the Appendix for the full VIPER algorithm.

3 Approach

We present two algorithms: IVIPER and MAVIPER. Both are general policy extraction algorithms for the multi-agent setting inspired by the single-agent VIPER algorithm. At a high level, given an expert policy profile $\pi^* = (\pi_1^*, \dots, \pi_N^*)$ with associated state-action value functions $Q^{\pi^*} = (Q_1^{\pi^*}, \dots, Q_N^{\pi^*})$ trained by an existing MARL algorithm, both algorithms apply a modified version of VIPER to produce a DT policy $\hat{\pi}_i$ for each agent i . These algorithms work with various state-of-art MARL algorithms, including value-based and multi-agent actor-critic methods. We first discuss IVIPER, the basic version of our multi-agent DT learning algorithm. We then introduce additional changes that form the full MAVIPER algorithm.

3.1 IVIPER

Motivated by the practical success of single-agent RL algorithms in the MARL setting [21,3], we extend single-agent VIPER to the multi-agent setting by independently applying the single-agent VIPER algorithm to each agent, with a few

critical changes described in detail below. Algorithm 1 shows the full pseudocode for our IVIPER algorithm.

First, we ensure that each agent has sufficient information for training its DT policy. Each agent has its own dataset \mathcal{D}_i of training tuples. When using VIPER with multi-agent actor-critic methods that leverage a per-agent centralized critic network Q_i^π , we ensure that each agent’s dataset \mathcal{D}_i has not only its observation and actions, but also the complete state information x — which consists of the observations of all of the agents — and the expert-labeled actions of all of the other agents $\pi_j^*(o_j) \forall j \neq i$. By providing each agent with the information about all other agents, we avoid the stationarity issue that arises when the policies of all agents are changing throughout the training process (like in MARL).

Second, we account for important changes induced by moving from a single-agent to a multi-agent formalism. When we sample and relabel trajectories for training each agent’s DT policy, we sample from the distribution $d^{\hat{\pi}_i^{m-1}, \pi_{-i}^*}$ induced by agent i ’s policy at the previous iteration $\hat{\pi}_i^{m-1}$ and the expert policies of all other agents π_{-i}^* . We only relabel the action for agent i because the other agents choose their actions according to expert policies π^* . It is equivalent to treating all other expert agents as part of the environment and only using DT policy for agent i .

Third, we need to account for the actions of all agents when resampling the dataset to construct a new, weighted dataset (Line 6, Algorithm 1). If the MARL algorithm uses a centralized critic $Q(s, \vec{a})$, we resample points according to:

$$p((x, a_1, \dots, a_N)) = \tilde{l}_i(x) \mathbb{I}[(x, a_1, \dots, a_N) \in \mathcal{D}_i], \quad (2)$$

where,

$$\tilde{l}_i(x) = V_i^{\pi^*}(x) - \min_{a_i \in \mathcal{A}_i} Q_i^{\pi^*}(x, a_i, \vec{a}_{-i}) \Big|_{\vec{a}_{-i} = \pi_j^*(o_j) \forall j \neq i}. \quad (3)$$

Crucially, we incorporate the actions of all other agents in Equation (3) to select agent i ’s minimum Q-value from its centralized state-action value function.

When applied to value-based methods, IVIPER is more similar to single-agent VIPER. In particular, in Line 4, Algorithm 1, it is sufficient to only store o_i and $\pi_i^*(o_i)$ in the dataset \mathcal{D}_i^m , although we still need to sample trajectories according to $\hat{\pi}_i^{m-1}$ and π_{-i}^* . In the resampling step in Line 6, we follow single-agent VIPER and use: $\tilde{l}_i(x) = V_i^{\pi^*}(s) - \min_{a_i \in \mathcal{A}_i} Q_i^{\pi^*}(o_i, a_i)$, removing the reliance of the loss on a centralized action-value function network.

Taken together, these algorithmic changes form the basis of the IVIPER algorithm. We note that this algorithm can be viewed as transforming the multi-agent learning problem to a single-agent one, in which other agents are treated as part of the environment. This approach works well if i) we only want an interpretable policy for a single agent in a multi-agent setting or ii) agents do not need to *coordinate* with each other. When coordination is needed, this algorithm does not reliably capture coordinated behaviors, as each DT is trained independently without consideration for what the other agent’s resulting DT policy will learn. This issue is particularly apparent when trees are constrained to have a small maximum depth, as is desired for interpretability.

3.2 MAVIPER

Algorithm 2 MAVIPER (Joint Training)

Input: (\mathcal{X}, A, P, R) , π^* , $Q^{\pi^*} = (Q_1^{\pi^*}, \dots, Q_N^{\pi^*})$, K , M
Output: $(\hat{\pi}_1, \dots, \hat{\pi}_N)$

- 1: Initialize dataset $\mathcal{D} \leftarrow \emptyset$ and policy for each agent $\hat{\pi}_i^0 \leftarrow \pi_i^* \forall i \in N$
 - 2: **for** $m = 1$ to M **do**
 - 3: Sample K trajectories: $\mathcal{D}^m \leftarrow \{(x, \pi_1^*(o_1), \dots, \pi_N^*(o_N)) \sim d^{(\hat{\pi}_1^{m-1}, \dots, \hat{\pi}_N^{m-1})}\}$
 - 4: Aggregate dataset $\mathcal{D} \leftarrow \mathcal{D} \cup \mathcal{D}^m$
 - 5: For each agent i , resample \mathcal{D}_i according to loss:
 $\mathcal{D}_i \leftarrow \{(x, \vec{a}) \sim p((x, \vec{a})) \propto \tilde{l}_i(x) \mathbb{I}[(x, \vec{a}) \in \mathcal{D}]\} \forall i \in N$
 - 6: Jointly train DTs: $(\hat{\pi}_1^m, \dots, \hat{\pi}_N^m) \leftarrow \text{TrainJointTrees}(\mathcal{D}_1, \dots, \mathcal{D}_N)$
 - 7: **return** Best set of agents $\hat{\pi} = (\hat{\pi}_1, \dots, \hat{\pi}_N) \in \{(\hat{\pi}_1^1, \dots, \hat{\pi}_N^1), \dots, (\hat{\pi}_1^M, \dots, \hat{\pi}_N^M)\}$

 - 8: **function** TRAINJOINTTREES($\mathcal{D}_1, \dots, \mathcal{D}_N$)
 - 9: Initialize decision trees $\hat{\pi}_1^m, \dots, \hat{\pi}_N^m$.
 - 10: **repeat**
 - 11: Grow one more level for agent i 's tree $\hat{\pi}_i^m \leftarrow \text{Build}(\hat{\pi}_1^m, \dots, \hat{\pi}_N^m, \mathcal{D}_i)$
 - 12: Move to the next agent: $i \leftarrow (i + 1) \% N$
 - 13: **until** all trees have grown to the maximum depth allowed
 - 14: **return** decision trees $\hat{\pi}_1^m, \dots, \hat{\pi}_N^m$

 - 15: **function** BUILD($\hat{\pi}_1^m, \dots, \hat{\pi}_N^m, \mathcal{D}_i$)
 - 16: **for** each data point $(x, \vec{a}) \in \mathcal{D}_i$ **do**
 - 17: // Will agent j 's (projected) final DT predict its action correctly?
 - 18: $v_j \leftarrow \mathbb{I}[\text{Predict}(\hat{\pi}_j^m, x) = a_j] \forall j \in [1, N]$
 - 19: // This data point is useful only if many agents' final DTs predict correctly.
 - 20: **if** $\sum_{j=1}^N v_j < \text{threshold}$ **then** Remove d from dataset: $\mathcal{D}_i \leftarrow \mathcal{D}_i \setminus \{(x, \vec{a})\}$
 - 21: $\hat{\pi}_i^m \leftarrow$ Calculate best next feature split for DT $\hat{\pi}_i^m$ using \mathcal{D}_i .
 - 22: **return** $\hat{\pi}_i^m$

 - 23: **function** PREDICT($\hat{\pi}_j^m, x$)
 - 24: Use x to traverse $\hat{\pi}_j^m$ until leaf node $l(x)$
 - 25: Train a projected final DT $\hat{\pi}'_j \leftarrow \text{TrainDecisionTree}(\mathcal{D}_j)$
 - 26: **return** $\pi.$ predict(x)
-

To address the issue of coordination, we propose MAVIPER, our novel algorithm for centralized training of coordinated multi-agent DT policies. For expository purpose, we describe MAVIPER in a fully cooperative setting and then explain how to use MAVIPER for mixed cooperative-competitive settings. At a high-level, MAVIPER trains all of the DT policies, one for each agent, in a centralized manner. It jointly grows the trees of each agent by predicting the behavior of the other agents in the environment using their anticipated trees. To train each DT policy, MAVIPER employs a new resampling technique to find

states that are critical for its interactions with other agents. The full MAVIPER algorithm is shown in Algorithm 2. Specifically, MAVIPER is built upon the following extensions to IVIPER that aim at addressing the issue of coordination.

First, in terms of resampling probability $p(\cdot)$, MAVIPER no longer calculates the probability $p(x)$ of a joint observation x by viewing the other agents as stationary experts. Instead, it considers the decision trees being trained at the moment, i.e., the adapting agents, and therefore we define the resampling probabilities used to construct the new dataset, as in Equation (2), using:

$$\tilde{l}_i(x) = \mathbb{E}_{\vec{a}_{-i}} \left[Q_i^{\pi^*}(x, \pi_i^*(x), \vec{a}_{-i}) - \min_{a_i \in \mathcal{A}_i} Q_i^{\pi^*}(x, a_i, \vec{a}_{-i}) \right]. \quad (4)$$

In accordance with this resampling probability, MAVIPER uses the DT policies $(\hat{\pi}_1^{m-1}, \dots, \hat{\pi}_N^{m-1})$ from the last iteration to perform rollouts and collect new data.

Second, we add a prediction module to the DT training process to increase the joint accuracy instead of the individual accuracy as in IVIPER, as shown in the **Predict** function. The prediction module aims at predicting the actions that the other decision trees $\{\hat{\pi}_j\}_{j \neq i}$ might make given their partial observations.

To make the most of the prediction module, MAVIPER grows the trees evenly using a breath-first ordering so that it will not be biased towards the result of any specific tree. Since the trees are not complete at the time of prediction, we use the output of a normal decision tree trained with the full dataset associated with that node as the prediction.

Using this prediction module, we are able to remove all data points whose proportion of correct predictions is lower than a predefined threshold, following the intuition that the correct prediction of one agent alone may not yield much benefit if the other agents are wrong. We can then calculate the splitting criteria based on this modified dataset, and further grow the tree in an iterative fashion.

In some mixed cooperative-competitive settings, agents in a team share goals and need to coordinate with each other, but they face other agents or other teams whose goals are not fully aligned with theirs. In these settings, MAVIPER follows a similar procedure to jointly train policies for agents in the same team to ensure coordination. More specifically, for a team Z , the **Build** and **Predict** function is constrained to only make predictions for the agents in the same team. Equation (4) now takes the expectation over the joint actions for agents outside the team and becomes:

$$\tilde{l}_i(x) = \mathbb{E}_{\vec{a}_{-Z}} \left[Q_i^{\pi^*}(x, \pi_i^*(x), \vec{a}_{-Z}) - \min_{a_i \in \mathcal{A}_i} Q_i^{\pi^*}(x, a_i, \vec{a}_{-Z}) \right]. \quad (5)$$

Taken together, these changes comprise the MAVIPER algorithm. Because we explicitly account for the anticipated behavior of other agents in both the predictions and the resampling probability, we hypothesize that MAVIPER should better capture coordinated behavior.

4 Experiments

We now investigate how well MAVIPER and IVIPER agents perform in a variety of environments. Because the goal is to learn high-performing yet interpretable policies, we evaluate the quality of the trained policies in three multi-agent environments: two mixed competitive-cooperative environments and one fully cooperative environment.

Since small DTs are considered interpretable, we constrain the maximum tree depth to be at most 6. The expert policies used to guide the DT training are generated by MADDPG [19] and we use the Pytorch [28] implementation*. We compare to two baselines:

1. Fitted Q-Iteration. We iteratively approximate the Q-function with a regression DT [8]. We derive the policy by taking the the action associated with the highest estimated Q-value for that input state.
2. Imitation DT. Each DT policy is directly trained using a dataset collected by running the expert policies for multiple episodes. No resampling is performed. The observations for an agent are the features, and the actions for that agent are the labels.

We detail the hyperparameters and the process for choosing these hyperparameters in Appendix B.3. We train a high-performing MADDPG expert, then run each DT-learning algorithm 10 times with different random seeds. We evaluate all policies by running 100 episodes.

4.1 Environments

We evaluate our algorithms on three multi-agent particle world environments [19], described below. Episodes terminate when the maximum number of timesteps $T = 25$ is reached. We choose the primary performance metric based on the environment (detailed below), and we also provide results using expected return as the performance metric in the Appendix.

Physical Deception. In this environment, a team of N defenders must protect N targets from one adversary. One of the targets is the true target, which is known to the defenders but not to the adversary. For our experiments, $N = 2$. Defenders succeed during an episode if they split up to cover all of the targets simultaneously; the adversary succeeds if it reaches the true target during the episode. Covering and reaching targets is defined as being ϵ -close to a target for at least one timestep during the episode. We use the defenders' and the adversary's success rate as the primary performance metric in this environment.

* <https://github.com/shariqiqbal2810/maddpg-pytorch>

Cooperative Navigation. This environment consists of a team of N agents, who must learn to cover all N targets while avoiding collisions with each other. For our experiments, $N = 3$. Agents succeed during an episode if they split up to cover all of the targets without colliding. Our primary performance metric is the summation of the distance of the closest agent to each target, for all targets. Low values of the metric indicate that the agents correctly learn to split up.

Predator-prey. This variant of the classic game involves a team of K slower, cooperating predators that chase M faster prey. There are also $L = 2$ large landmarks impeding the way. For our experiments, $K = M = 2$. We assume that each agent has a restricted observation space consisting primarily of binarized relative positions and velocity (if applicable) of the landmarks and other agents in the environment. For full details, see Appendix B.1. Our primary performance metric is the number of collisions between predators and prey. For prey, lower is better; for predators, higher is better.

4.2 Results

For each environment, we compare the DT policies generated by different methods and check if MAVIPER and MAVIPER agents achieve better performance ratio than the baselines overall. We also investigate whether MAVIPER learns better coordinated behavior than IVIPER. Furthermore, we investigate which algorithms are the most robust to different types of opponents. We conclude with an ablation study to determine which components of the MAVIPER algorithm contribute most to its success.

Individual Performance Compared to Experts We analyze the performance of the DT policies when only one agent adopts the DT policy while all other agents use the expert policies. Given a DT policy profile $\hat{\pi}$ and the expert policy profile π^* , if agent i who belongs to team Z uses its DT policy, then the individual performance ratio is defined as:

$$\text{Individual performance ratio} = \frac{U_Z(\hat{\pi}_i, \pi_{-i}^*)}{U_Z(\pi^*)}, \quad (6)$$

where $U_Z(\cdot)$ is team Z 's performance given the agents' policy profile since we define our primary performance metrics at the team level. A performance ratio of 1 means that the DT policies perform as well as the expert ones. We can get a ratio above 1, since we compare the performance of the DT and the expert policies in the environment, not the similarity of the DT and expert policies.

We report the mean individual performance ratio for each team in Figure 1, averaged over all trials and all agents in the team. The error bars show the 95% confidence interval.

As shown in Figure 1a, individual MAVIPER and IVIPER defenders outperform the two baselines for all maximum depths in the physical deception environment. However, MAVIPER and IVIPER adversaries perform similarly

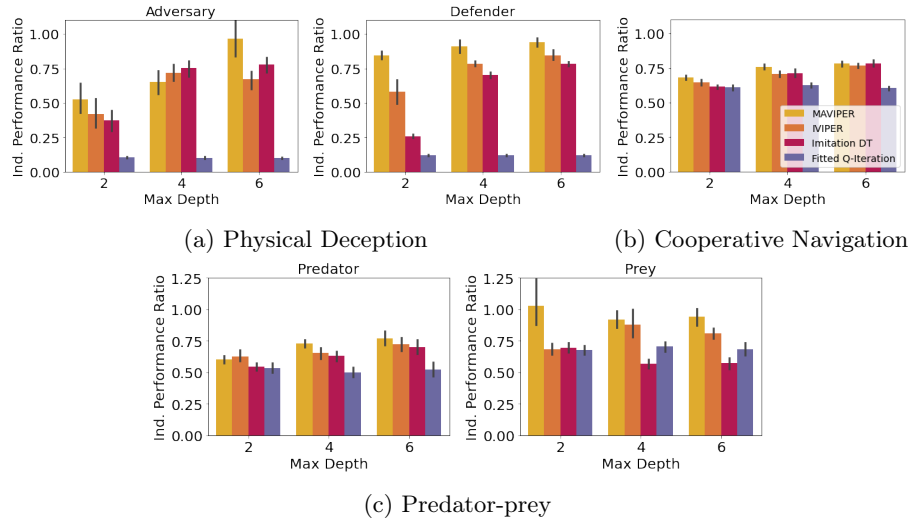


Fig. 1: Individual performance ratio: Relative performance when only one agent adopts DT policy and all other agents use expert policy.

to the Imitation DT adversary, indicating that the correct strategy may be simple enough to capture with a less-sophisticated algorithm. Agents also perform similarly on the cooperative navigation environment (Figure 1b). As mentioned in the original MADDPG paper [19], this environment has a less stark contrast between success and failure, so these results are not unexpected.

In predator-prey, we see the most notable performance difference when comparing the prey. When the maximum depth is 2, only MAVIPER achieves near-expert performance. When the maximum depths are 4 and 6, MAVIPER and IVIPER agents achieve similar performance and significantly outperform the baselines. The predators achieve similar performance across all algorithms. We suspect that the complexity of this environment makes it challenging to replace even a single predator’s policy with a DT.

Furthermore, MAVIPER achieves a performance ratio above 0.75 in all environments with a maximum depth of 6. The same is true for IVIPER, except for the adversaries in physical deception. That means DT policies generated by IVIPER and MAVIPER lead to a performance degradation of less than or around 20% compared to the less interpretable NN-based expert policies. These results show that IVIPER and MAVIPER generate reasonable DT policies and outperform the baselines overall when adopted by a single agent.

Joint Performance Compared to Experts A crucial aspect in multi-agent environment is the coordination among agents, especially when agents are in the same team with shared goals. To ensure that the DT policies capture this desired behavior, we analyze the performance of the DT policies when all agents

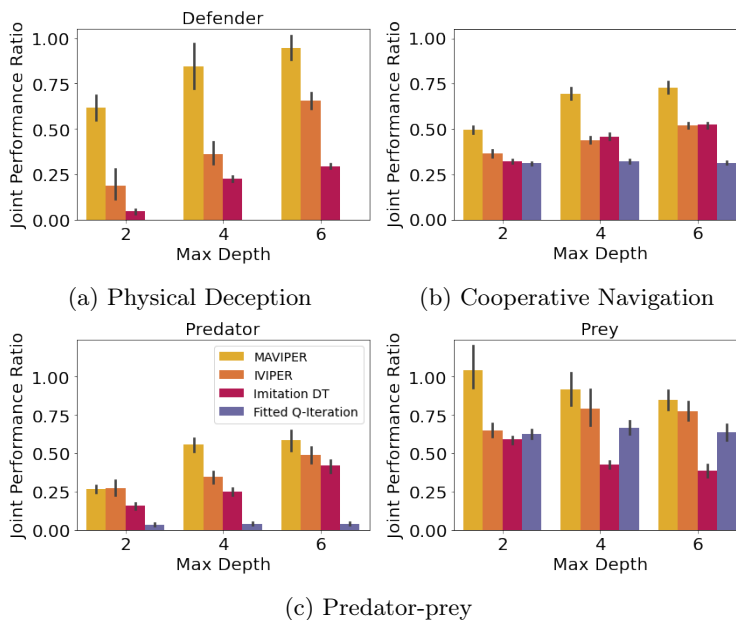


Fig. 2: Joint performance ratio: Relative performance when all agents in a team adopt DT policy and other agents use expert policy.

in a team adopt DT policies, while other agents use expert policies. The joint performance ratio is defined as:

$$\text{Joint performance ratio} = \frac{U_Z(\hat{\pi}_Z, \pi_{-Z}^*)}{U_Z(\pi^*)},$$

where $U_Z(\hat{\pi}_Z, \pi_{-Z}^*)$ is the utility of team Z when using their DT policies against the expert policies of the other agents $-Z$. We report the mean joint performance ratio for each team, averaged over all trials in Figure 2. The error bars show the 95% confidence interval.

Figure 2a shows that MAVIPER defenders outperform IVIPER and the baselines, indicating that it better captures the coordinated behavior necessary to succeed in this environment. Fitted Q-Iteration struggles to achieve coordinated behavior in this environment, despite obtaining non-zero success for individual agents. This algorithm cannot capture the coordinated behavior, which we suspect is due to poor Q-value estimates. We hypothesize that the superior performance of MAVIPER is partially due to the defender agents correctly splitting their “attention” to the two targets to induce the correct behavior of covering both targets. To investigate this, we inspect the normalized average feature importances of the DT policies of depth 4 for both IVIPER and MAVIPER over 5 of the trials, as shown in Figure 3. Each of the MAVIPER defenders (top) most commonly focuses on the attributes associated with one of the targets. More

specifically, defender 1 focuses on target 2 and defender 2 focuses on target 1. In contrast, both IVIPER defenders (bottom) mostly focus on the attributes associated with the goal target. Not only does this overlap in feature space mean that defenders are unlikely to capture the correct covering behavior, it also leaves them more vulnerable to an adversary, as it is easier to infer the correct target.

Figure 2b shows that MAVIPER agents significantly outperform all other algorithms in the cooperative navigation environment for all maximum depths. IVIPER agents significantly outperform the baselines for a maximum depth of 2, but achieve similar performance to the Imitation DT for the other maximum depths, where both algorithms significantly outperform the Fitted Q-Iteration baseline. Taken together, these results indicate that MAVIPER better captures coordinated behavior, even as we increase the complexity of the cooperation problem by introducing another cooperating agent.

Figure 2c shows that the prey team trained by IVIPER and MAVIPER only outperform the baselines for all maximum depths. The team of predators trained by IVIPER and MAVIPER similarly outperform the baselines for all maximum depths. Also, MAVIPER leads to better performance than IVIPER in two of the settings (prey with depth 2 and predator with depth 4) while having no statistically significant advantage in other settings.

Taken together, these results indicate that IVIPER and MAVIPER can better capture the coordinated behavior necessary for a team to succeed in different environments compared to the baselines, with MAVIPER significantly outperforming IVIPER in several environments.

Robustness to Different Opponents We now investigate the robustness of the DT policies when a team using DT policies play against a variety of opponents in the mixed competitive-cooperative environments: physical deception and predator-prey. For this set of experiments, we choose a maximum depth of 4. Given a DT policy profile $\hat{\pi}$, a team Z 's performance against an alternative policy file π' used by the opponents is defined as

$$\text{Team performance against opponent } \pi' = U_Z(\hat{\pi}_Z, \pi'_{-Z}),$$

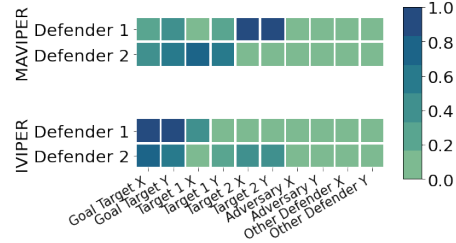


Fig. 3: Features used by the two defenders in the physical deception environment. Features are relative positions of that agent and the labeled feature. Darker squares correspond to more importance placed on that feature. MAVIPER defenders most commonly split importance across the two targets.

Environment	Team	MAVIPER	IVIPER	Imitation DT	Fitted Q-Iteration
Physical Deception	Defender	.78 (.16)	.33 (.09)	.24 (.19)	.01 (.01)
	Adversary	.42 (.03)	.41 (.03)	.42 (.04)	.07 (.01)
Predator-prey	Predator	2.37 (0.67)	1.87 (0.53)	1.16 (0.30)	0.17 (0.13)
	Prey	1.76 (0.82)	1.78 (1.07)	2.69 (1.91)	1.93 (1.28)

Table 1: Robustness results. We report mean team performance and standard deviation of DT policies for each team, averaged across a variety of opponent policies. The best-performing algorithm for each agent type is shown in **bold**.

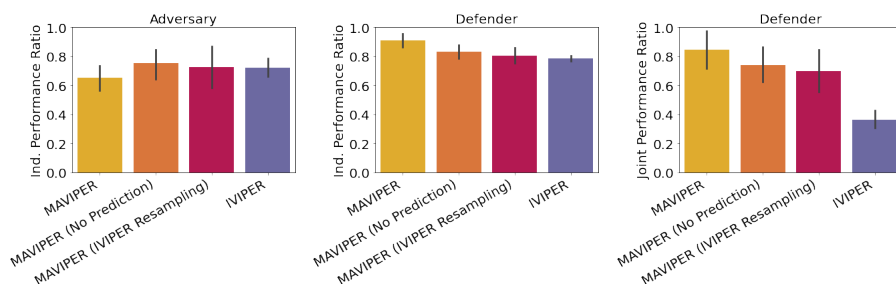


Fig. 4: Ablation study for MAVIPER for a maximum depth of 4. MAVIPER (No Prediction) does not utilize the predicted behavior of the anticipated DTs of the other agents to grow each agent’s tree. MAVIPER (IIVPER Resampling) uses the same resampling method as IVIPER.

We consider a broad set of opponent policies π' , including the policies generated by MAVIPER, IVIPER, Imitation DT, Fitted Q-Iteration, and MADDPG. We report the mean team performance for each team, averaged over all opponent policies, in Table 1. For the full results, see Table 4 and Table 3 in Appendix C.

For physical deception, MAVIPER defenders outperform all other algorithms, with a gap of .45 between its performance and the next-best algorithm, IVIPER. This result indicates that MAVIPER learns coordinated defender policies that perform well against a variety of adversaries. On the adversary side, MAVIPER, IVIPER, and Imitation DT adversaries all perform similarly on average, with a similar standard deviation. This result supports the idea that the adversary’s desired behavior is simplistic enough to capture with a less sophisticated algorithm.

For predator-prey, MAVIPER predators and prey perform the best compared to all other algorithms. Due to the complexity of this environment, the standard deviation of the performance of all algorithms is high.

Ablation Study As discussed in Section 3.2, MAVIPER makes a few critical changes compared to IVIPER to improve the coordination among agents in a

team. In particular, we utilize the predicted behavior of the anticipated DTs of the other agents to grow each agent’s tree. We also alter the resampling probability (Equation (4)) to incorporate the average Q-values over all actions for the other agents. To investigate the contribution of these changes to the performance, we run an ablation study with a maximum depth of 4 on the physical deception environment. We report the mean independent performance ratio and the mean joint performance ratio for the defender team in Figure Section 4.2, comparing MAVIPER and IVIPER to two variants of MAVIPER without one of the two critical changes. Results show that both changes contributed to the improvement of MAVIPER over IVIPER, especially in the joint performance ratio. The error bars show the 95% confidence interval.

5 Related Work

Most work on interpretable RL focuses on the single-agent setting [23]. We first discuss techniques that directly learn DT policies. CUSTARD [39] extends the action space of the MDP to contain actions for constructing a DT, i.e., choosing a feature to branch a node. Training an agent in the augmented MDP yields a DT policy for the original MDP while still enabling training using any function approximator, like NNs, during training. By redefining the MDP, the learning problem becomes more complex, which can be problematic in multi-agent settings where the learning problem is already made more complicated due to the presence of other agents. A few other works focus on directly learning DT policies [8,22,41] for single-agent RL but not for the purpose of interpretability. Further, these works have custom learning algorithms and cannot utilize a high-performing NN policy to guide training.

VIPER [2] is considered to be a post-hoc DT-learning method [2]; however, we use it to produce *intrinsically* interpretable policies for deployment. MOET [42] extends VIPER by learning a mixture of DT policies trained on different regions of the state space. The resulting policy is a linear combination of multiple trees with non-axis-parallel partitions of the state. We find that the performance difference between VIPER and MOET is not significant enough to increase the complexity of the policy structure, which would sacrifice interpretability.

Despite increased interest in interpretable single-agent RL, interpretable MARL is less commonly explored. One line of work generates explanations from potentially non-interpretable policies. For example, some recent work uses attention [13,16,26] to select and focus on critical factors that impact agents in the training process. Other work generates explanations in the form of verbal explanations with predefined rules [44] or Shapley values [11]. The most similar line of work to ours focuses on model extraction [14], in which non-interpretable policies of MARL agents are approximated to interpretable ones using the framework of abstract argumentation. This work constructs argument preference graphs given manually-provided arguments. In contrast, our work does not need these manually-provided arguments for interpretability. Instead, we generate DT policies.

6 Discussion and Conclusion

We proposed IVIPER and MAVIPER, the first algorithms, to our knowledge, that train interpretable DT policies for MARL. We evaluated these algorithms on both cooperative and mixed competitive-cooperative environments. We showed that they can achieve individual performance of at least 75% of expert performance in most environment settings and over 90% in some of them, given a maximum tree depth of 6. We also empirically validated that MAVIPER effectively captures coordinated behavior by showing that teams of MAVIPER-trained agents outperform the agents trained by IVIPER and several baselines. We further showed that MAVIPER generally produces more robust agents than the other DT-learning algorithms.

Future work includes learning these high-quality DT policies from fewer samples, e.g., by using dataset distillation [43]. We also note that our algorithms can work in some environments where the experts and DTs are trained on different sets of features. Since DTs can be easier to learn with a simpler set of features, future work includes augmenting our algorithm with an automatic feature selection and engineering component that constructs simplified yet still interpretable features for training the DT policies.

References

1. Abbeel, P., Ng, A.: Apprenticeship learning via inverse reinforcement learning. In: ICML (2004)
2. Bastani, O., et al.: Verifiable reinforcement learning via policy extraction. In: NeurIPS (2018)
3. Berner, C., et al.: Dota 2 with large scale deep reinforcement learning. arXiv preprint 1912.06680 (2019)
4. Bhalla, S., et al.: Deep multi agent reinforcement learning for autonomous driving. In: Canadian Conf. Artif. Intell. (2020)
5. Brittain, M., Wei, P.: Autonomous air traffic controller: A deep multi-agent reinforcement learning approach. arXiv preprint arXiv:1905.01303 (2019)
6. Buciluă, C., et al.: Model compression. In: KDD (2006)
7. Degris, T., et al.: Learning the structure of factored Markov decision processes in reinforcement learning problems. In: ICML (2006)
8. Ernst, D., et al.: Tree-based batch mode reinforcement learning. JMLR **6** (2005)
9. Foerster, J., et al.: Stabilising experience replay for deep multi-agent reinforcement learning. In: ICML (2017)
10. Foerster, J., et al.: Counterfactual multi-agent policy gradients. In: AAAI (2018)
11. Heuillet, A., et al.: Collective explainable ai: Explaining cooperative strategies and agent contribution in multiagent reinforcement learning with shapley values. IEEE Comput. Intell. Magazine **17** (2022)
12. Hinton, G., et al.: Distilling the knowledge in a neural network. arXiv preprint arXiv:1503.02531 (2015)
13. Iqbal, S., Sha, F.: Actor-attention-critic for multi-agent reinforcement learning. In: ICML (2019)
14. Kazhdan, D., et al.: Marleme: A multi-agent reinforcement learning model extraction library. In: IJCNN (2020)

15. Li, S., et al.: Robust multi-agent reinforcement learning via minimax deep deterministic policy gradient. In: AAAI (2019)
16. Li, W., et al.: Sparsemaac: Sparse attention for multi-agent reinforcement learning. In: Int. Conf. Database Syst. for Adv. Appl. (2019)
17. Lipton, Z.: The mythos of model interpretability. *ACM Queue* **16**(3) (2018)
18. Littman, M.: Markov games as a framework for multi-agent reinforcement learning. In: *Mach. Learning* (1994)
19. Lowe, R., et al.: Multi-agent actor-critic for mixed cooperative-competitive environments. *arXiv preprint arXiv:1706.02275* (2017)
20. Malialis, K., Kudenko, D.: Distributed response to network intrusions using multiagent reinforcement learning. *Eng. Appl. Artif. Intell.* (2015)
21. Matignon, L., et al.: Independent reinforcement learners in cooperative markov games: a survey regarding coordination problems. *Knowledge Eng. Review* **27**(1) (2012)
22. McCallum, R.: Reinforcement learning with selective perception and hidden state. PhD Thesis, Univ. Rochester, Dept. of Comp. Sci. (1997)
23. Milani, S., et al.: A survey of explainable reinforcement learning. *arXiv preprint arXiv:2202.08434* (2022)
24. Mohanty, S., et al.: Flatland-rl: Multi-agent reinforcement learning on trains. *arXiv preprint arXiv:2012.05893* (2020)
25. Molnar, C.: *Interpretable Machine Learning* (2019)
26. Motokawa, Y., Sugawara, T.: Mat-dqn: Toward interpretable multi-agent deep reinforcement learning for coordinated activities. In: ICANN (2021)
27. Oliehoek, F., et al.: Optimal and approximate q-value functions for decentralized pomdps. *JAIR* **32** (2008)
28. Paszke, A., et al.: Automatic differentiation in pytorch (2017)
29. Pyeatt, L.: Reinforcement learning with decision trees. In: *Appl. Informatics* (2003)
30. Pyeatt, L., Howe, A.: Decision tree function approximation in reinforcement learning. In: *Int. Symp. on Adaptive Syst.: Evol. Comput. and Prob. Graphical Models* (2001)
31. Quinlan, J.: *Induction of decision trees*. *Mach. Learning* (1986)
32. Rashid, T., et al.: Qmix: Monotonic value function factorisation for deep multi-agent reinforcement learning. In: ICML (2018)
33. Ross, S., et al.: A reduction of imitation learning and structured prediction to no-regret online learning. In: AISTATS (2011)
34. Roth, A., et al.: Conservative q-improvement: Reinforcement learning for an interpretable decision-tree policy. *arXiv preprint arXiv:1907.01180* (2019)
35. Shapley, L.: Stochastic games. *PNAS* **39**(10) (1953)
36. Son, K., et al.: Qtran: Learning to factorize with transformation for cooperative multi-agent reinforcement learning. *arXiv preprint arXiv:1905.05408* (2019)
37. Strehl, A., et al.: Efficient structure learning in factored-state mdps. In: AAAI (2007)
38. Sunehag, P., et al.: Value-decomposition networks for cooperative multi-agent learning. *arXiv preprint arXiv:1706.05296* (2017)
39. Topin, N., et al.: Iterative bounding mdps: Learning interpretable policies via non-interpretable methods. In: AAAI (2021)
40. Tuyls, K., et al.: Reinforcement learning in large state spaces. In: *Robot Soccer World Cup* (2002)
41. Uther, W., Veloso, M.: The lumberjack algorithm for learning linked decision forests. In: *Int. Symp. Abstract., Reformulation, and Approx.* (2000)

42. Vasic, M., et al.: Moët: Interpretable and verifiable reinforcement learning via mixture of expert trees. arXiv preprint arXiv:1906.06717 (2019)
43. Wang, T., et al.: Dataset distillation. arXiv preprint arXiv:1811.10959 (2018)
44. Wang, X., et al.: Explanation of reinforcement learning model in dynamic multi-agent system. arXiv preprint arXiv:2008.01508 (2020)
45. Yu, C., et al.: The surprising effectiveness of mapo in cooperative, multi-agent games. arXiv preprint arXiv:2103.01955 (2021)

Algorithm 3 VIPER for Single-Agent Setting

Input: $(S, A, P, R), \pi^*, Q^*, K, M$ **Output:** $\hat{\pi}$

- 1: Initialize dataset $\mathcal{D} \leftarrow \emptyset$
 - 2: Initialize policy $\hat{\pi}^0 \leftarrow \pi^*$
 - 3: **for** $m = 1$ to M **do**
 - 4: Sample K trajectories:
 $\mathcal{D}^m \leftarrow \{(s, \pi^*(s)) \sim d^{\hat{\pi}^{m-1}}\}$
 - 5: Aggregate dataset $\mathcal{D} \leftarrow \mathcal{D} \cup \mathcal{D}^m$
 - 6: Resample dataset according to loss:
 $\mathcal{D}' \leftarrow \{(s, a) \sim p((s, a)) \propto \tilde{l}(s) \mathbb{I}[(s, a) \in \mathcal{D}]\}$
 - 7: Train decision tree $\hat{\pi}^m \leftarrow \text{TrainDecisionTree}(\mathcal{D}')$
 - 8: **return** Best policy $\hat{\pi} \in \{\hat{\pi}^1, \dots, \hat{\pi}^M\}$ on cross validation
-

A Omitted Algorithm

Algorithm 3 shows the full pseudocode for the single-agent version of VIPER [2].

B Experimental Details

B.1 Environments

For all environments, we utilize the initialization and reward scheme as described in the original MADDPG paper [19] and Pytorch implementation. The only change we make is to the predator-prey environment, which we describe below.

Predator-prey. We follow the definition of the original environment proposed in the multi-agent particle environment [19], with only changes in the partial observation provided to each agent. The observations of the adversary and the agents consist of the concatenation of the following vectors:

1. [self_pos, self_vel]
2. binarized relative positions and relative velocity (if applicable) of the landmarks and other agents using $\text{sgn}(x)$ as the binarizing function
3. binarized relative distance between all pairs of agents on the other team. If the opponent team has agent a_1, a_2 , then it will be $[\text{sgn}(x_1 - x_2), \text{sgn}(y_1 - y_2)]$.
4. binarized relative distance between all pairs of agents on the same team.

For an environment with $K = M = 2$, the observation size will be 22 and 24 respectively for the adversary and the agents.

B.2 Implementation Details

To optimize running speed, MAVIPER adopts a caching mechanism to avoid training a new decision tree for each data point being predicted. It also does

Algorithm	Environment	Max Training Iterations	Number of Rollouts	Threshold	Max Samples
IVIPER	Physical	50	50		
	Deception				
	Cooperative	100	50	N/A	300,000
	Navigation				
	Predator-prey	100	100		
MAVIPER	All	100	50	$N - 1$	300,000
Imitation DT	All	20	N/A	N/A	100,000
Fitted Q-Iteration	All	10	N/A	N/A	100,000

Table 2: Hyperparameter values used for all algorithms.

parallelization for the `Predict` function starting from Line 23 by precomputing all the prediction information upfront, where the each prediction is delayed until all data points are looped over. In this way, MAVIPER can gather all the predictions that a particular tree needs to make and therefore do it in a parallel manner.

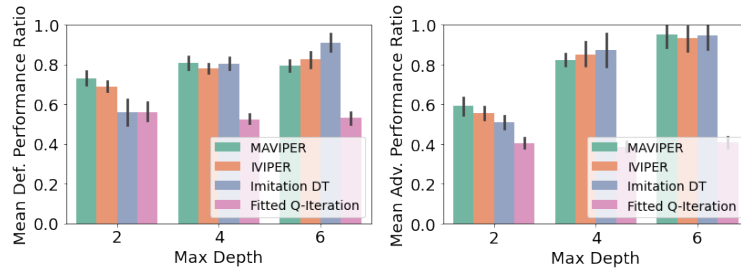
Since IVIPER is fully decentralized, training of each DT can be performed in parallel.

B.3 Hyperparameters

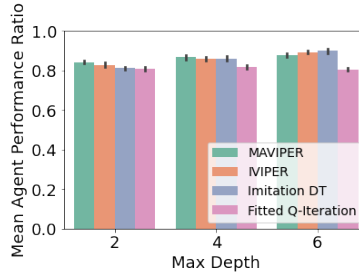
We vary the hyperparameters that would impact training performance of these algorithms 2-3 times and choose the hyperparameters that yield the agents with the best performance. For all environments, we vary the number of rollouts to be $[50, 100]$ and the number of iterations to be $[30, 100]$, while the threshold is fixed at $N - 1$. For the baselines, we also vary the maximum number of samples used for training each agent between $[10000, 30000, 100000]$. For Imitation DT, we did not see much of a performance increase between 30000 and 100000 samples, so we pick the maximum value for fairness of comparison. Table 2 shows the values of the hyperparameters that are utilized by all algorithms. Although we set a maximum number of training iterations for MAVIPER, we stop training early when there is no noticeable performance gain to further improve runtime.

C Additional Results

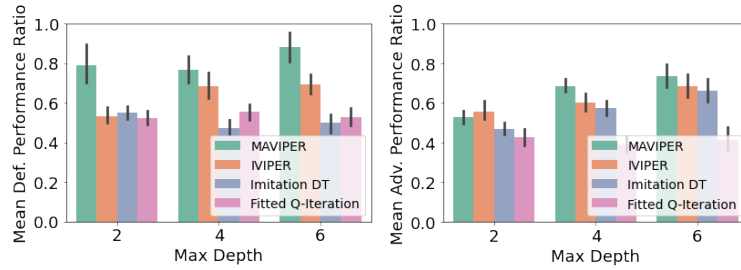
In Appendices C.1 and C.2, we further present results using the defined environment reward. This reward is not as intuitive as the primary metric for many of these environments, but we present the results here for the sake of completeness. The individual and joint performance ratios are defined in the same way as in Section 4.2 in the main body of the paper, with one caveat. Since we are now measuring reward, which may be negative or positive, we take $\frac{||A|-|B||}{A}$ to report how much more or less B is than A .



(a) Physical Deception



(b) Cooperative Navigation



(c) Predator-prey

Fig. 5: Individual performance ratio measured by reward. Individual performance ratio, measured by reward, of DT agents compared to expert agents for different maximum depths. Higher is better. Error bars represent the 95% confidence interval.

C.1 Individual Performance

Figure 5 shows the individual performance ratio measured by reward on all three environments.

Physical Deception Results for physical deception are shown in Figure 5a. Interestingly, MAVIPER and IVIPER defenders only significantly outperform both baselines when the maximum depth is 2. When the maximum depth is 4, MAVIPER, IVIPER, and Imitation DT perform similarly, with Fitted Q-Iteration barely

reaching above .50 for all depths. When the maximum depth is 6, Imitation DT actually achieves the highest defender reward, significantly outperforming all other algorithms. However, as shown in Figure 1 in the main body, MAVIPER significantly outperforms all algorithms for all maximum depths when reporting the success ratio. This is because the reward is in part dependent on the performance of the adversary. In other words, a poorly-performing defender can achieve similar performance to a high-performing defender if the poor-performing defender is paired with a high-performing adversary. We see a similar pattern for the adversary performance: IVIPER, MAVIPER, and Fitted Q-Iteration all significantly outperform the Fitted Q-Iteration baseline for different maximum depths. We note that MAVIPER tends to perform better for lower maximum depths, which is desirable for interpretability.

Cooperative Navigation Results for cooperative navigation are shown in Figure 5b. IVIPER and MAVIPER significantly outperform the Fitted Q-Iteration baseline for all maximum depths. However, MAVIPER only significantly outperforms Imitation DT when the maximum depth is 2. Otherwise, IVIPER, MAVIPER, and Imitation DT all perform similarly.

Predator-prey Results for predator-prey are shown in Figure 5c. MAVIPER prey significantly outperform all other algorithms for maximum depths of 2 and 6. For a maximum depth of 4, MAVIPER and IVIPER algorithms both significantly outperform the baselines. In contrast, MAVIPER predators only significantly outperform all other algorithms for a maximum depth of 4. For a maximum depth of 2, MAVIPER and IVIPER significantly outperform the baselines, For a maximum of depth of 6, MAVIPER, IVIPER, and Imitation DT significantly outperform Fitted Q-Iteration. Again, we note that this performance is not necessarily reflected in the results using the collision metric in Figure 1c.

C.2 Joint Performance

Figure 6 shows the joint performance ratio measured by reward on all three environments.

Physical Deception Figure 6a shows the results on physical deception. MAVIPER defenders significantly outperform all other algorithms on this environment for maximum depths of 2 and 4. For a maximum depth of 6, IVIPER, MAVIPER, and Imitation DT all perform similarly. Note that MAVIPER again achieves good performance for lower maximum depths, demonstrating its promise as an algorithm for producing interpretable policies. We also note that, again, the reward metric is somewhat deceptive: when measuring the success conditions in the environment (as in Figure 2 in the main body of the paper), MAVIPER significantly outperforms all other algorithms for all maximum depths.

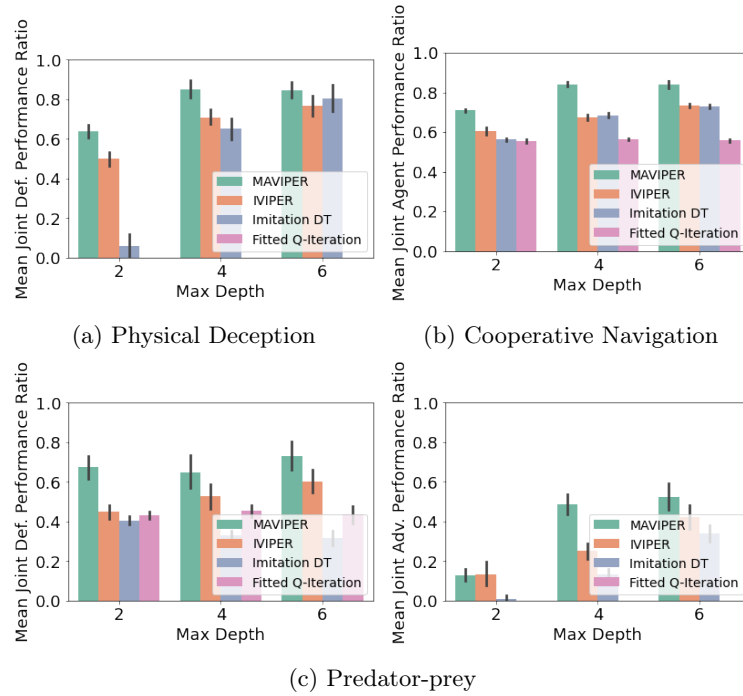


Fig. 6: Joint performance ratio, measured by reward, of DT agents compared to expert agents for different maximum depths. DT agents are evaluated jointly. Error bars represent the 95% confidence interval. Higher is better.

Cooperative Navigation Figure 6b depicts the joint agent performance on the cooperative navigation environment. Interestingly, we see that MAVIPER significantly outperforms all other algorithms for all maximum depths, despite obtaining similar individual performance. Consequently, this means that MAVIPER better captures the desired coordinated behavior than all of the other algorithms.

Predator-prey Figure 6c shows the results for the predator-prey environment. MAVIPER prey significantly outperform other algorithms for a maximum depth of 2. For maximum depths of 6 and 8, it achieves slightly better (but not statistically significant) performance than IVIPER, and significantly outperforms the two baselines. MAVIPER and IVIPER predators enjoy similar performance for maximum depths of 2 and 6. For a maximum depth of 4, MAVIPER significantly outperforms all other algorithms. Note that the correct behavior in this environment is challenging to capture with a small decision tree, as the number of features is either 22 or 24, depending on the agent type.

Predator	Prey				
	MAVIPER	IVIPER	Imitation DT	Fitted Q-Iteration	MADDPG
MAVIPER	(2.28 , 2.28)	(3.49 , 3.49)	(2.41 , 2.41)	(2.32 , 2.32)	(1.37 , 1.37)
IVIPER	(1.95, 1.95)	(2.46, 2.46)	(2.17, 2.17)	(1.89, 1.89)	(0.88, 0.88)
Imitation DT	(1.32, 1.32)	(1.17, 1.17)	(1.18, 1.18)	(1.53, 1.53)	(0.61, 0.61)
Fitted Q-Iteration	(0.42, 0.42)	(0.18, 0.18)	(0.14, 0.14)	(0.02, 0.02)	(0.11, 0.11)
MADDPG	(2.78, 2.78)	(3.36, 3.36)	(5.82, 5.82)	(3.85, 3.85)	(2.54, 2.54)

Table 3: Robustness results of DT agents on predator-prey. Results are presented as: average number of touches in an episode. Higher is better for predator, and lower is better for prey. Excluding MADDPG, the best-performing prey (lowest in value) for each predator type is in **blue** and the best-performing predator (highest in value) for each prey type is in **red**.

C.3 Robustness to Different Opponents

We present the full robustness results for the predator-prey and physical deception environments. For space reasons, we only report the average over the 100 trials; however, we only label the best-performing agent of each type in either **red** or **blue** if the 95% confidence intervals do not overlap, unless otherwise mentioned. We exclude MADDPG from this calculation, since we know that MADDPG agents will outperform all other agent types, and we are mostly interested in how well the *decision tree* policies perform.

Predator-prey MAVIPER predators are strictly more robust than all other agents (except MADDPG) to different types of prey. MAVIPER prey are the most or second most robust to different types of predators. In this environment, predator coordination is more critical, as predators must strategically catch the prey. The prey, on the other hand, does not require much coordination, which explains the Imitation DT prey’s robustness by imitating the action of the single-agent expert.

Physical Deception MAVIPER defenders are the most robust than all agents (except MADDPG) to different types of adversaries. Interestingly, MAVIPER, IVIPER, and Imitation DT adversaries all perform similarly. Indeed, they often do not achieve performance that is statistically significant from one another, as measured by the 95% confidence interval. However, we still highlight the best-performing adversary in **red** to more easily show the attained performance. Note that MADDPG adversaries can occasionally achieve success greater than around .50, which means that these adversaries can take advantage of some information about the defenders to correctly choose the target to visit. In contrast, adversaries trained with any of the DT-learning algorithms never achieve greater than .50, which indicates that they may need a more complex representation to capture important details about the defenders.

Adversary	Defender				
	MAVIPER	IVIPER	Imitation DT	Fitted Q-Iteration	MADDPG
	MAVIPER	(.42, .76)	(.45, .33)	(.45, .23)	(.37, .01)
IVIPER	(.39, .78)	(.45, .32)	(.40, .23)	(.36, .01)	(.43, .92)
Imitation DT	(.40, .79)	(.42, .34)	(.46, .26)	(.36, .01)	(.46, .92)
Fitted Q-Iteration	(.07, .80)	(.07, .34)	(.07, .21)	(.06, .00)	(.06, .90)
MADDPG	(.71, .76)	(.77, .32)	(.77, .26)	(.53, .00)	(.62, .90)

Table 4: Robustness results of DT agents on physical deception. Results are presented as: (adversary success ratio, defender success ratio). Higher is better. Excluding MADDPG, the best-performing defender for each adversary type is in blue and the best-performing adversary for each defender type is in red.

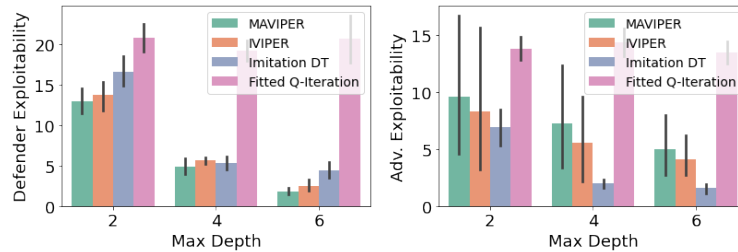


Fig. 7: Exploitability of DT defenders and adversaries in the physical deception environment. Lower exploitability is better.

C.4 Exploitability

In this set of experiments, we evaluate the exploitability of DT policies in the physical deception environment. Formally, we define the exploitability of a team Z as:

$$\text{Exploitability of team } Z = \max_{\pi'_{-Z}} U_{-Z}(\pi_Z, \pi'_{-Z}) - U_{-Z}(\pi_Z, \pi_{-Z}), \quad (7)$$

where the optimal π'_{-Z} is the best response policy profile to team Z 's policies. Practically, to measure exploitability, we fix the policies of the agents in team Z under evaluation and calculate its approximate best response π'_{-Z} by training a new neural network policy to convergence using MADDPG.

We evaluate the exploitability of the adversary and defenders in the physical deception environment and report the results in Figure 7. For the defending team, MAVIPER exhibits the lowest exploitability on all three depths, showing its effectiveness in learning coordinated policies. It is worth noting that in such a multi-agent learning setting, Imitation DT no longer performs well due to the complexity of the expert and the necessity of cooperation between agents. For the adversary, Imitation DT performs well while IVIPER and MAVIPER performs

similarly as the second best. This could be the result that imitation learning quickly imitates a near-optimal expert adversary starting from the depth of four. Since the adversary consists of only a single agent, MAVIPER and IVIPER are reduced to the same method.